

# A Molecular Dynamics Simulation of the Influence of Defect on the Melting of Amorphous Silica

Haijun Ji<sup>1</sup>, Xiaofang Wang<sup>1</sup>, Huiran Li<sup>1\*</sup>, Zhiyuan Li<sup>1</sup> and Xinlu Cheng<sup>2,3</sup>

<sup>1</sup>Equipment Support Department, Logistics University Of People's Armed Police Force, No.1, Huizhi Ring Road, Dongli District, Tianjin, China

<sup>2</sup>Institute of Atomic and Molecular Physics, Sichuan University, No.24, South Part of First Ring Road, Wuhou District, Chengdu, China

<sup>3</sup>Key Laboratory of High Energy Density Physics and Technology of Ministry of Education, Sichuan University, No.24, South Part of First Ring Road, Wuhou district, Chengdu, China

**Keywords:** Molecular dynamics simulation; The vacancy cluster; Amorphous silica

**Abstract:** In this paper, the influence of defect on the melting process of amorphous silica has been studied using molecular dynamics simulations. Using the bond evolution, it can be found that the melting process is intimately related to the formation of defect. Meanwhile, there are some differences in the melting process between the defected and undefected amorphous silica models. In addition, the pre-existing defect (void) contributes to the damage of SiO<sub>2</sub> materials. And the glass transition temperature can be effectively reduced, when the defects meet certain concentration.

## 1 INTRODUCTION

Silica is an important material in the technical engineering. Vitreous silica is the most usual structure among the various configuration states. For this reason, amorphous silica (Bates, 1972; Huff et al., 1999; Takada et al., 2004; Zachariassen, 1932; Afify et al., 2017; Peek et al., 2018) has been widely investigated. For instance, through the experimental observation, Zhang *et al.* (Zhang, et al., 1993) studied the effects of pressure on the melting of SiO<sub>2</sub>, and provided the glass transition temperatures under different pressures. As for the theoretical research, the molecular dynamics (MD) has been used to produce the vitreous silica by direct heating  $\beta$ -cristobalite (El-Sayed et al., 2013; Mukhopadhyay et al., 2004; Roder et al., 2001; Vollmayr et al., 1996). Hoang (Hoang et al., 2007) investigates the structures and thermodynamic properties for the varisized vitreous silica using MD method.

When the silica material exposes to the radiation (Gusev, 2000; Kurkjian, 2000; Kang et al., 2008; Blöchl, 2000; Kuo et al., 2006; Zhang et al., 2008; Malavasi et al., 2006), the vacancies may be formed in the bulk. In turn the vacancies can lead to the degradation of material properties. It has been found that the motion of defects in the SiO<sub>2</sub> material might

cause serious device problems (Fowler, et al., 1997). Luo *et al.* (An et al., 2006; Luo et al., 2007) pointed that defect-induced densification of silica glass is the dominant mechanism for densification. And the vacancies can induce densification of silica glass (An et al., 2006; Luo et al., 2007). In addition, according to the previous reports, if there is a sufficient concentration, vacancies tend to cluster and form voids (Zheng et al., 2006; Weber et al., 1998). Therefore, the silica with various vacancies attracts a lot of attention and has been studied using the MD method (An et al., 2006; Luo et al., 2007; Mota et al., 2008). We can find a lot of work, which were performed to investigate the materials with voids in the past years (Chan and Elliott, 1991; Mitra and Hockney, 1980). Malavasi *et al.* (Malavasi et al., 2006) studied void size distribution in silica glass structures.

In line with this, we focus on investigating the effect of defect on the melting process of silica glass. Especially, the effect of the particular defect, vacancy cluster (void), is considered in our study. Because the reactive force field (ReaxFF) (van Duin et al., 2001) developed by Duin (van Duin, 2009) is the tailored force field for a particular chemical reaction (Rimsza et al., 2018; Chenoweth et al., 2008). ReaxFF has been able to provide reasonable accuracy for observable various phenomena,

including the properties of the SiO<sub>2</sub> polymorphs (Cowen et al., 2016), oxidation of silicon carbide (Newsome et al., 2012), catalytic selective oxidation processes (Chenoweth et al., 2008) and the effect of an applied electric field (Assowe et al., 2012; Wood et al., 2004; Gubbels- Elzas et al., 2014; Hattori et al., 2012). Meanwhile, the ref. (Yu et al., 2016) points that the ReaxFF can offer a realistic description of silica glass. Considering all of these, MD and the ReaxFF are applied in our simulations. In order to study the influence of void, we construct the models with pre-existing structural defect for amorphous silica, respectively. With the purpose of revealing the insightful physical and chemical details, detailed structural analyses are provided in the melting process.

## 2 CALCULATION METHOD

The initial structure of amorphous silica used in our MD simulations is presented in Figure 1. The angle parameters of the used primitive cell are  $\alpha = \beta = \gamma = 90^\circ$ , and the length parameters are  $a=b=c = 21.39486 \text{ \AA}$ . The density of the intact construction is  $2.20 \text{ g/cm}^3$ . The simulation box of amorphous silica is constructed as  $2a \times 2b \times 2c$  superlattice (with 5184 atoms). On the basis of ref. (An et al., 2006) and (Luo et al., 2007), the defective models are constructed by removing atom clusters. The atom cluster with 21 atoms is removed from the intact amorphous silica to construct the model with a void. For convenience, the defected structure is labeled as a-defect1. While the atom cluster with 76 atoms are also eliminated to build the other defected silica, which is named as a-defect2. Totally, there are two kinds of defected silica (a-defect1 and a-defect2) constructed, which has the defect concentration 0.41% and 1.47%, respectively. Moreover, each of the void is located near the center of the system. Additionally, the intact amorphous silica is defined as a-intact. To clearly understand the progress of structural damaging, the constructions are divided into three regions from inside to outside, which can be seen in Figure 1. For the defected models, the introduced vacancy cluster is located in the region 1.

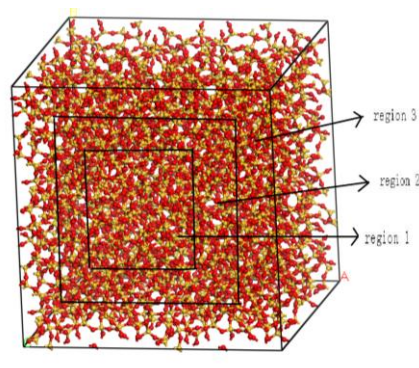


Figure 1: Schematic of the simulated system amorphous silica, the yellow and red spheres indicate Si and O atoms, respectively.

Considering the capability of the description of silicon oxides, the force field parameters expanded by Newsome *et al.* (Newsome et al., 2012) are used in our work. To verify the feasibility of the force field parameters, the Si–O bond of  $\beta$ -cristobalite is calculated. The average length for the initial Si–O bond provided by the ReaxFF is  $1.58 \text{ \AA}$ . It is in agreement with the length,  $1.55 \text{ \AA}$ , in the idealized structure. Therefore, the force field parameters expanded by Newsome *et al.* are suited for the study of the SiO<sub>2</sub> materials.

At the same time, three dimensional periodic conditions are applied in all of the MD simulations, which are performed with the LAMMPS software package (Plimpton, 1995). During the entire simulation process, the time step is set as  $0.2 \text{ fs}$  to integrate the equations of motion. As for the ensemble, both of the canonical (NVT) ensemble and micro-canonical (NVE) ensemble are used in our calculations. Firstly, the configurations are equilibrated at  $300 \text{ K}$  for  $10 \text{ ps}$  using the canonical (NVT) ensemble. Then the temperature for all of the systems experiences a linear growth, and the heating rate is  $1.675 \text{ K/ps}$ . The temperature is controlled using a Berendsen thermostat (Berendsen et al., 1984), with a temperature damping constant of  $10\text{fs}$ . The micro-canonical (NVE) ensemble is used in the heating process. In this case, we can make a comparison in the potential energy between different models under the same thermal growth rate and target temperature. To characterize the progress in detail, we make an analysis of bonds evolution. At the same time, the root mean square displacement (RMSD) is also computed during the simulation.

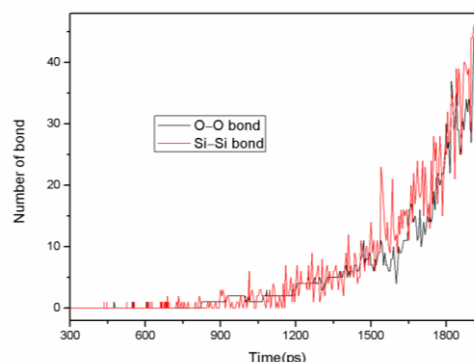
### 3 RESULTS AND DISCUSSION

#### 3.1 The Bond Evolution

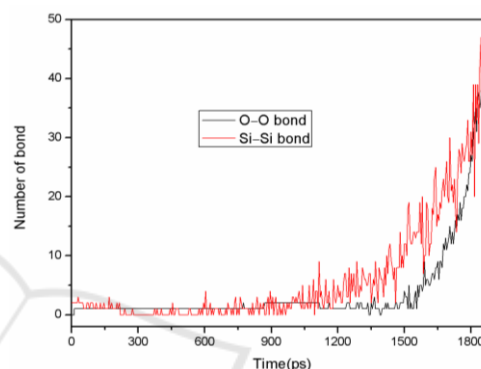
It is well known that the melting of solid state requires to break structural bonds, accompanied by the formation of new bonds. Since the bonds are localized, the number of bonds directly reflects the formation and dissociation of bonds (the bonding dynamic). It is necessary to make a detailed analysis of bond evolution in melting process. When the distance between two atoms is more than  $3 \text{ \AA}$ , there is almost no interaction. Considering this, it is can be regarded as a Si–Si or O–O bond, if the distance of two Si atoms or two O atoms is less than  $3 \text{ \AA}$ . On the basis, the changes of Si–Si and O–O bonds are analyzed in the simulations.

Figure 2 displays the calculated number of Si–Si and O–O bonds in amorphous silica over time. From Figure 2(a), it can be noted that there are no Si–Si and O–O bonds in the initial intact silica. Both of them appear as individually new bonds in the melting process. Then, the number of the new bonds tends to increase with the time running. It reveals that the damage of the bulk of amorphous silica stems from the formation of individual new bonds in the heating process.

Meanwhile, the evolution of Si–Si and O–O bonds gives an inspection for the occurrence of structural defects, such as vacancy defect and interstitial defect. We notice that the formation of Si–Si bond is earlier than that of O–O bond. Then it explains that Si atom escapes from its initial lattice site at first. However, the number of bond experiences a fluctuation with the time running, which illustrates the newly formed bonds can also be broken. The reason may be that the escaped atoms are free and randomly displace. During the diffusion, they might bond to the other atoms except for their initial first-neighbour atoms. Correspondingly, the Si–Si and O–O bonds are formed and broken. As a result, various defects are involved into the melting material. We can also obtain the melting mechanism, the melting process is intimately related to the individual defect.



(a)



(b)

Figure 2: The number of Si–Si and O–O bonds over time in the intact amorphous silica and (b) the a-defect2.

According to Figure 2(b), there is a Si–Si bond in a-defect2, when it begins to heat the material. It accounts that the Si–Si bond exists in equilibrium state of a-defect2. At the same time, the increasing of Si–Si bond is faster than that of a-intact. And the O–O bond appears once the heating time reaches 13 ps. Obviously, the appearance of O–O bond is earlier than the undefected structure. It suggests that the atoms are less stable and the old bonds (Si–O bonds) are more easier to be destroyed, when the void is introduced into amorphous silica. It also demonstrates that the defect helps to destroy the material. Additionally, Similar to the case of intact amorphous silica, newly formed Si–Si and O–O bonds also can be broken in heating process.

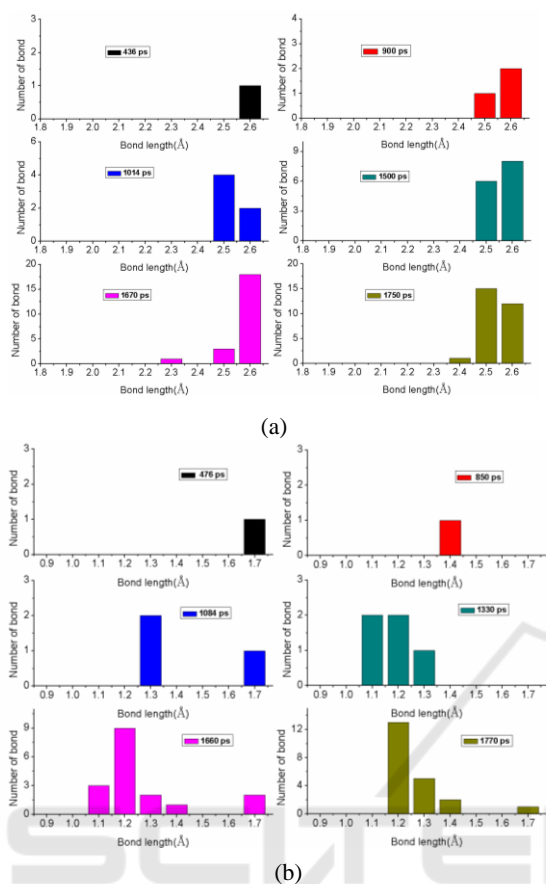


Figure 3: At some chosen time, the distribution of bond length, (a) Si-Si and (b) O-O, in the melting process of intact amorphous silica.

The bond distribution for intact amorphous silica demonstrates that the Si-Si and O-O bonds are generated with a long bond length at the initial stage (in Figure 3). With the time running, there is an expansion in the bond distribution. After some time, the Si-Si bond lengths are mainly around 2.5 Å–2.6 Å. And the bond lengths of O-O concentrate in the range from 1.2 Å to 1.3 Å. It can be deduced that the strength of newly formed bond is weak at the low temperature (because the temperature continuously rises over time).

### 3.2 The Potential Energy

Figure 4 presents the changes of potential energies in the heating process. There are some differences in the evolutions of the potential curves for the three models. When the void is introduced into amorphous silica structures, the materials will have higher potential energies. The reason maybe that the atoms around the void are less stable. Moreover, with the time running, there is an increase in the

potential energy of SiO<sub>2</sub> material, including the void-structural material.

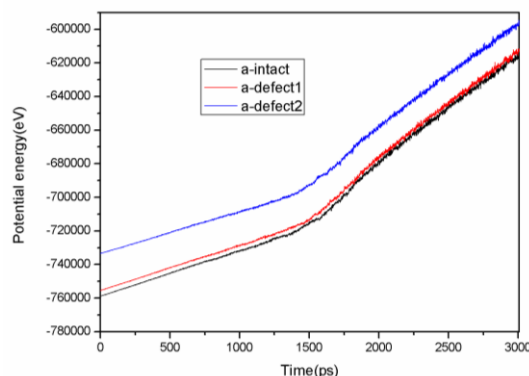


Figure 4: The potential energy change for different models of amorphous silica.

Figure 4 shows an inflection point in the potential curve of amorphous silica with or without pre-existing structural defect. But the variation in the slope of curve is not very markedness. The reason is simply that the amorphous silica presents a disordered state. While the abrupt increase maybe directly correlative with the melting of the material.

### 3.3 The RMSD

The calculated RMSDs for the defected and undefected models are shown in Figure 5. Obviously, there are noticeable differences in the shape of RMSD curves for a-intact, a-defect1 and a-defect2. Obviously, the different defect concentrations can lead to various growth rate in the RMSD of amorphous silica models. There is a higher growth rate in the RMSDs of a-defect1 and a-defect2. For example, the RMSDs of a-intact, a-defect1 and a-defect2 reaches 1 Å at the time of 1179 ps, 1154 ps, 1089 ps, respectively. The RMSD of a-defect2 increases more quickly than that of a-intact and a-defect1. It indicates that RMSD changes faster with the increase of defect concentration. We can speculate that it is more easier to be destroyed, when there is higher defect concentrations.

According to the Lindemann criterion (Lindemann et al., 1910), melting occurs when the RMSD of the atoms reaches a critical fraction of the interatomic distance. And it has been used to study the melting temperature in the normal thermodynamic melting (Gilvarry et al., 1988; Ubbelohda, 1978). At the same time, Jin *et al.* (Jin et al., 2001) pointed out that the RMSD value at the glass transition temperature is about ~ 0.22 times of the interatomic distance. On basis of this, the glass

transition temperature of amorphous silica is predicted. The bond length statistics shows that the average Si–O bond length in the initial intact amorphous silica is 1.60 Å, as well as the defected models. Therefore, for amorphous silica, the RMSD of the atoms at the glass transition temperature is  $\sim 0.352$  Å. Therefore, the progress of structural melting can be obtained by observing the RMSD.

All of the RMSDs for a-intact, a-defect1 and a-defect2 reach 0.353 Å, at the time of 908 ps, 925 ps, 776 ps, respectively. Combining with the calculated temperature, the glass transition temperature is estimated to be 1812.6 K, 1846.4 K and 1587.8 K, for the intact amorphous silica, a-defect1 and a-defect2, respectively. Comparing with the value of the other two amorphous silica models, when the defect concentration is 1.47%, the glass transition temperature can be significantly decreased, which is reduced by about 12.4%. It explains that the glass transition temperature can be effectively reduced, when the defects meet certain concentration.

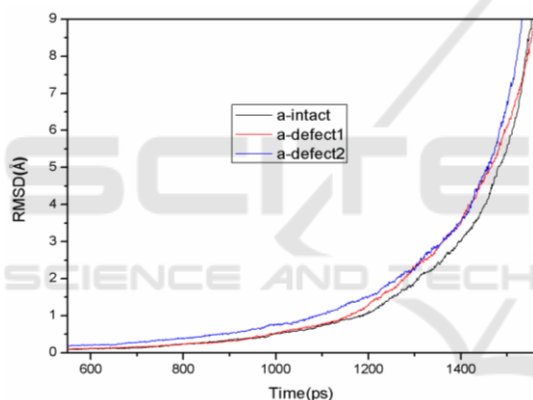


Figure 5: RMSD for the defected and undefected system.

From Figure 5, we can see that there are some overlapping locations in a-intact and a-defect1. In addition, the missing atomicity of a-defect1 is less, comparing with a-defect2. The RMSDs for the three regions of a-defect2, which has higher defect concentration, are analyzed and compared as illustrated in Figure 6.

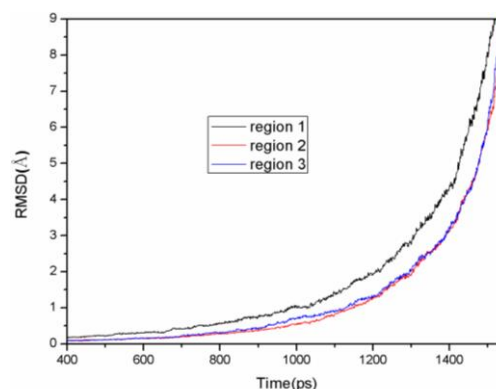


Figure 6: RMSD for the three regions in the model of a-defect2.

Figure 6 demonstrates that the RMSDs for the three regions of a-defect2 have sudden changes at different time. Apparently, the atoms in the defective region (region 1) diffuse at first. When the system is further heated, the atoms in the region 2 and region 3 start to diffuse. And the RMSD value for the defected region also has a faster increase with the time running. According to the Lindemann criterion, we can speculate that the melting phenomenon of a-defect2 begins at the defect center. At the same time, the RMSD changes with time for region 2 and region 3 is similar with each other. The reason maybe that there is a relatively small number of atoms in region 2 during the partitioning of a-defect2.

#### 4 SUMMARY AND CONCLUSIONS

In our MD simulations, the force field parameters expanded by Newsome *et al.* are used to study the melting processes of amorphous silica materials. By analyzing the Si–Si and O–O bonds evolution, we find that the number of bond tends to increase with the time running, when the Si–Si or O–O bond appears as a newly formed bond. Comparing with the bond evolution, it can be noticed that there are some differences in the melting processes of the amorphous silica models. Moreover, the analysis of bond evolution gives an inspection for the occurrence of structural defect in the melting process. Our calculation results suggest that the damage of the SiO<sub>2</sub> materials stems from the migration of O or Si atom during the heating process. And it also provides the melting mechanism, i.e. the melting process is intimately related to the formation of defect. Additionally, the sequence of

events demonstrates that the defects contribute to the melting of SiO<sub>2</sub> materials.

Attribute to the presence of the void, there is a higher potential energy for both of a-defect1 and a-defect2. The glass transition temperature is estimated to be 1812.6 K, 1846.4 K and 1587.8 K, for a-intact, a-defect1 and a-defect2, respectively. While the introduced of the defect concentration 1.47% makes the glass transition temperature reduce by about 12.4%. From this calculated RMSD, we can know that the vacancy cluster can reduce the glass transition temperature of the material to a certain extent.

## ACKNOWLEDGEMENTS

We thank the financial support from the National Natural Science Foundation of China (NSAF. Grant No. 11176020 and NSFC. Grant No. 11374217).

## REFERENCES

- Afify, N.D., Mountjoy G., Haworth R., 2017. *Comput. Mater. Sci.* 128: 75.
- An Q., Zheng L., Luo S. -N., 2006. *J. Non-Cryst. Solids* 352: 3320.
- Assowe O., Politano O., Vignal V., Arnoux P., Diawara B., Verners O., van Duin A. C. T., 2012. *J. Phys. Chem. A* 116: 11796.
- Bates, J. B., 1972. *J. Chem. Phys.* 57: 4042.
- Berendsen, H. J. C., Postma, J. P. M., Van Gunsteren, W. F., Dinola, A., Haak, J. R., 1984. *J. Chem. Phys.* 81: 3684.
- Blöchl, P.E., 2000. *Phys. Rev. B* 62: 6158.
- Chan, S. L., Elliott, S. R., 1991. *Phys. Rev. B* 43: 4423.
- Chenoweth, K., Van Duin, A. C. T., Persson, P., Cheng, M. J., Ongaard, J., Goddard, W. A., III, 2008. *J. Chem. Phys. C* 112: 14645.
- Cowen, B. J., Ei-Genk, M. S., 2016. *Comput. Mater. Sci.* 111: 269.
- El-Sayed, A., Watkins, M. B., Shluger, A. L., Afanas'ev V. V., 2013. *Microelectron. Eng.* 109: 68.
- Fowler, W. B., Edwards, A. H., 1997. *J. Non-Cryst. Solids* 222: 33.
- Gilvary, J. J., 1956. *Phys. Rev.* 102: 308; Voronel A., Rabinovitch S., Kisliuk A., Steinberg V., Sverbilova T., 1988. *Phys. Rev. Lett.*, 60: 2402.
- Gubbels-Elzas, A., Thijssse, B. J., 2014. *Comput. Mater. Sci.* 90: 196.
- Gusev, E.P., 2000. in: G. Pacchioni, L. Skuja, D. Griscom (Eds.), *NATO Science Series, Kluwer Academic Press, Dordrecht* 557.
- Hattori, S., Kalia, R. K., Nakano, A., Nomura, K., Vashishta, P., 2012. *Appl. Phys. Lett.* 101: 063106.
- Hoang, V. V., 2007. *J. Phys. Chem. B* 111: 12649–12656.
- Huff, N. T., Demiralp, E., Cagin, T., Goddard III, W. A., 1999. *J. Non-Cryst. Solids* 253: 133.
- Jin, Z. H., Gumbsch, P., Lu, K., Ma, E., 2001. *Phys. Rev. B* 87: 055703-1.
- Kang J., Kim Y. -H., Bang J., Chang K. J., 2008. *Phys. Rev. B* 77: 195321.
- Kuo, C. -L., Hwang, G. S., 2006. *Phys. Rev. Lett.* 97: 066101.
- Kurkjian, C. R., Krol, D. M., 2000. in: R.B. Devine, J.-P. Duraud, E. Dooryheé (Eds.), *John Wiley and Sons, New York* 449.
- Lindemann, F. A., *Phys. Z.*, 1910. *Physikalische Zeitschrift der Sowjetunion* 11: 609–612.
- Luo, S. -N., Zheng, L., An, Q., Wu, H. -A., Xia, K., Ni, S., 2007. *Proc. SPIE* 6403: 64030C-1.
- Malavasi, G., Menziani, M. C., Pedone, A., Segre, U., 2006. *J. Non-Cryst. Solids* 352: 285.
- Mitra, S. K., Hockney, R. W., 1980. *J. Phys. C: Sol. Stat. Phys.* 13: L739.
- Mota, F., Molla, J., Caturla, M. -J., Ibarra, A., Perlado, J. M., 2008. *J. Phys.: Conf. Ser.* 112: 032032.
- Mukhopadhyay, S., Sushko, P. V., Stoneham, A. M., Shluger, A. L., 2004. *Phys. Rev. B* 70: 195203.
- Newsome, D. A., Sengupta, D., Foroutan, H., Russo, M. F., van Duin, A. C. T., 2012. *J. Phys. Chem. C* 116: 16111.
- Peek, N.M., Jeffcoat, D.B., et al., 2018. *J. Phys. Chem. C* 122: 4349.
- Plimpton, S., 1995. *J. Comput. Phys.* 117: 1.
- Rimsza, J. M., Jones, R. E., Criscenti, L. J., 2018. *J. Colloid. Interface Sci.* 516: 128.
- Roder, A., Kob, W., Binder, K., 2001. *J. Chem. Phys.* 114: 7602.
- Takada, A., Richet, P., Catlow, C.R.A., Price, G.D., 2004. *J. Non-Cryst. Solids* 345–346: 224.
- Ubbelohda, A. R., 1978. *Wiley, Chichester*.
- van Duin, A. C. T., 2009. [http://www.wag.caltech.edu/home/duin/reax\\_um.pdf](http://www.wag.caltech.edu/home/duin/reax_um.pdf).
- van Duin, A. C. T., Dasgupta, S., Lorant, F., Goddard, W. A., III, 2001. *J. Phys. Chem. A* 105: 9396.
- Vollmayr, K., Kob, W., Binder, K., 1996. *Phys. Rev. B* 54: 15808.
- Weber, W. J. et al., 1998. *J. Mater. Res.* 13: 1434.
- Wood, M. A., van Duin, A. C. T., Strachan, A., 2014. *J. Phys. Chem. A* 118: 885.
- Yu, Y., Wang, B., et al., 2016. *J. Non-Cryst. Solids* 443: 148.
- Zachariasen, W.H., 1932. *J. Am. Chem. Soc.* 54: 3841.
- Zhang, G., Li, X., Tung, C. -H., Pey, K. -L., Lo, G. -Q., 2008. *Appl. Phys. Lett.* 93: 022901.
- Zhang, J., Liebermann, R. C., Gasparik T., et al., 1993. *J. Geophys. Res. Solid Earth* 98: 19785.
- Zheng, L., An, Q., Fu, R., Ni, S., Luo, S. -N., 2006. *J. Chem. Phys.* 125: 154511.